Electronic Supplementary Material (ESI) for Physical Chemistry Chemical Physics.

Electronic Supplementary Information

Giant photonic spin Hall effect induced by hyperbolic shear polaritons

Guangyi Jia,[1,*] Wenxuan Xue,[1] Zhenxin Jia,[1] Mathias Schubert[2,†]

[1]School of Science, Tianjin University of Commerce, Tianjin 300134, P. R. China

[2]Department of Electrical and Computer Engineering, University of Nebraska-Lincoln, Lincoln, Nebraska 68588, USA

E-mails: *gyjia87@163.com; †schubert@engr.unl.edu

Calculation method for the permittivity tensor of β-Ga_2O_3

The β-Ga_2O_3 monoclinic permittivity elements consist of the high-frequency contributions, the dipole charge resonances, and the free charge-carrier contributions, which can be calculated by the following equations

$$\varepsilon_{xx} = \varepsilon_{\infty,xx} + \sum_{j=1}^{8} \rho_{j,B_u} \sin^2 \alpha_j + \vartheta_{FCC,x} \tag{S1}$$

$$\varepsilon_{yy} = \varepsilon_{\infty,yy} + \sum_{j=1}^{8} \rho_{j,B_u} \sin^2 \alpha_j + \vartheta_{FCC,y} \tag{S2}$$

$$\varepsilon_{zz} = \varepsilon_{\infty,zz} + \sum_{j=1}^{4} \rho_{j,A_u} + \vartheta_{FCC,z} \tag{S3}$$

$$\varepsilon_{xy} = \varepsilon_{yx} = \varepsilon_{\infty,xy} + \sum_{j=1}^{8} \rho_{j,B_u} \sin \alpha_j \cos \alpha_j \tag{S4}$$

where ε_∞ is the permittivity at high frequency for different directions, the A_u and B_u are long-wavelength active modes (infrared and far-infrared); the A_u modes are polarized along axis b only and the B_u modes are polarized within the a-c plane. The factor α_j is the angle between the dipole oscillation axis of B_u mode j and the axis a of the β-Ga_2O_3 crystal. The 8(4) modes mean that this material has 8(4) long-wave active intrinsic modes of vibration for the B_u (A_u) modes. The Lorentzian-broadened oscillator function $\rho_{j,(Au,Bu)}$ stands for the energy-dependent contribution to the long-wavelength polarization response of an uncoupled electric dipole charge oscillation of B_u mode j (A_u mode j). The Drude model function ϑ_{FCC} gives the energy-dependent contribution to the long-wavelength polarization response of free charge carriers for different directions. The Drude model function ϑ_{FCC} and the Lorentzian-broadened oscillator function $\rho_{j,(Au,Bu)}$ can be expressed as

$$\vartheta_{FCC,(x,y,z)} = \frac{e^2 N}{\varepsilon_0 m_{eff,(z,y,z)}\omega\left(\omega + i\gamma_{p,(x,y,z)}\right)} \tag{S5}$$

$$\rho_{j,(A_u,B_u)} = \frac{A_{j,(A_u,B_u)}}{\omega^2_{TO,[j,(A_u,B_u)]} - \omega^2 - i\omega\kappa_{j,(A_u,B_u)}} \tag{S6}$$

Here, N is the free charge-carrier density. $m_{eff,(x,y,z)}$ and $\gamma_{p,(x,y,z)}$ are the electron effective mass and the damping coefficient along different directions, respectively. ε_0 is the permittivity in vacuum, and e is the amount of the electrical unit charge. $A_{j,(Au,Bu)}$, $\omega_{TO,[j,(Au,Bu)]}$, and $\kappa_{j,(Au,Bu)}$ indicate the amplitude, resonance frequency, and broadening parameter of a lattice resonance with transverse optical (TO) character for A_u mode j or B_u mode j. The β-Ga_2O_3 monoclinic crystals are electron doped by different free charge-carrier densities N with increasing $\log_{10}N$ from 18.0 to 19.4. The specific parametrization and computational details are available in ref. 22 in the main article.

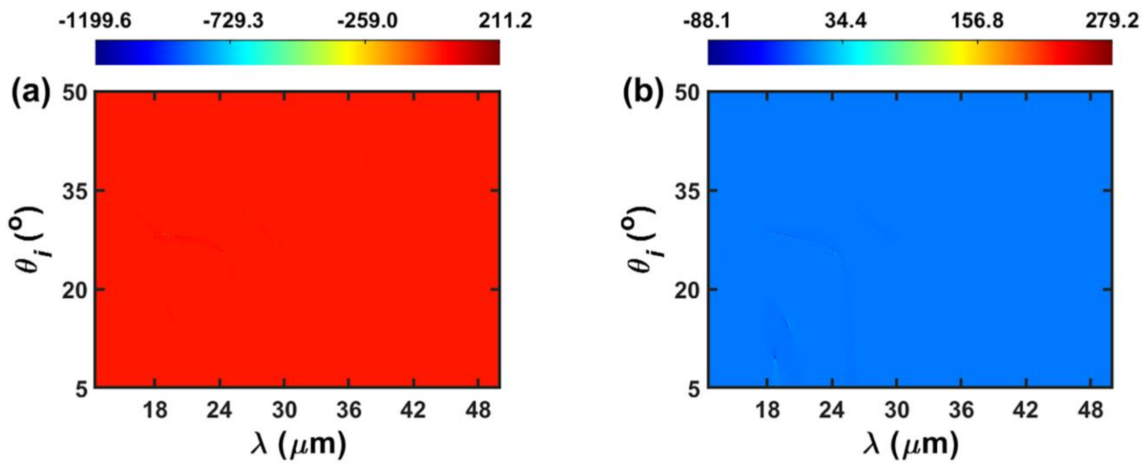

Fig. S1 Original color maps of Fig. 3(c) and (d). (a) In-plane and (b) transverse spin-dependent shifts versus the parameters of θ_i and λ. The color bars are scaled in the unit of λ.

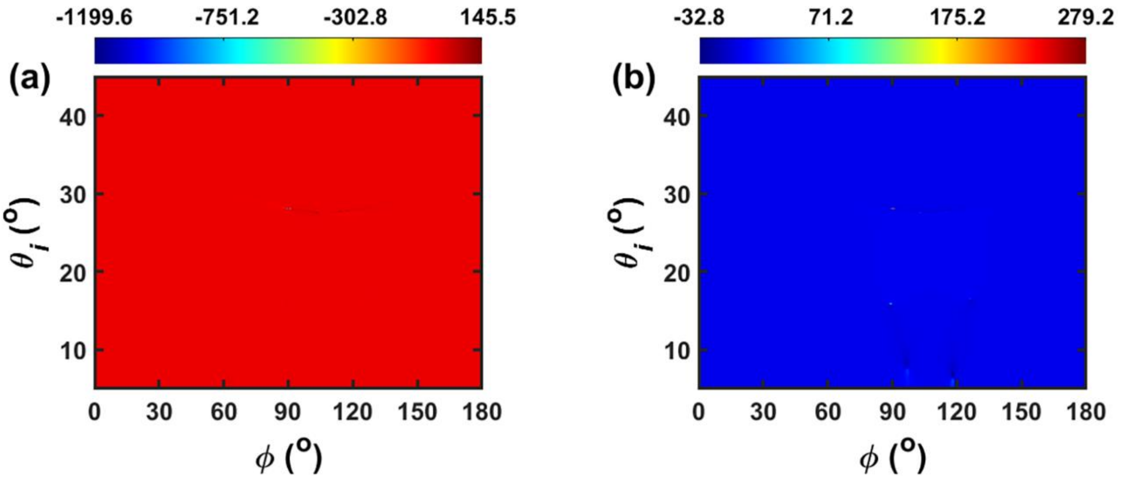

Fig. S2 Original color maps of Fig. 6(c) and (d). (a) In-plane and (b) transverse spin-dependent shifts versus the parameters of θ_i and ϕ. The color bars are scaled in the unit of λ.

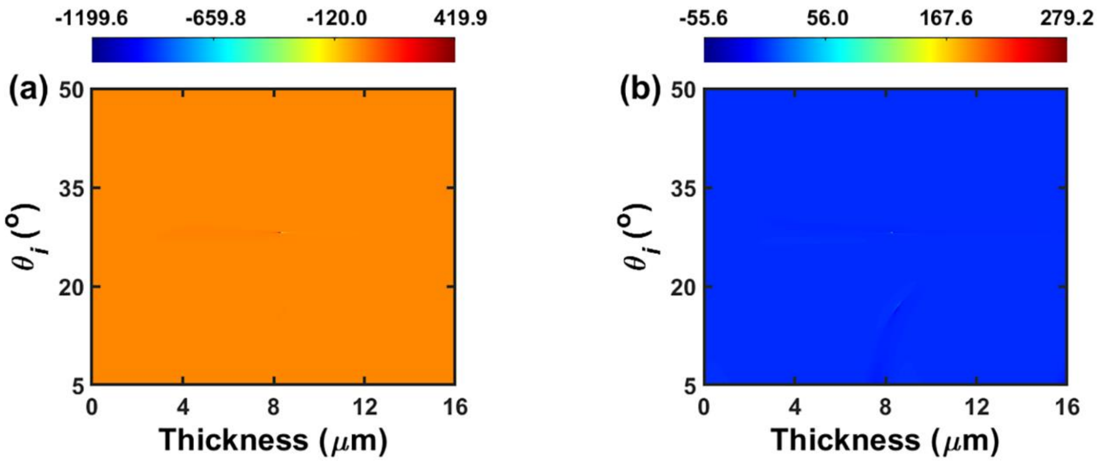

Fig. S3 Original color maps of Fig. 7(c) and (d). (a) In-plane and (b) transverse spin-dependent shifts versus the incident angle and the thickness of biosensing medium. The refractive index of biosensing medium is n_s = 1.419. The color bars are scaled in the unit of λ.

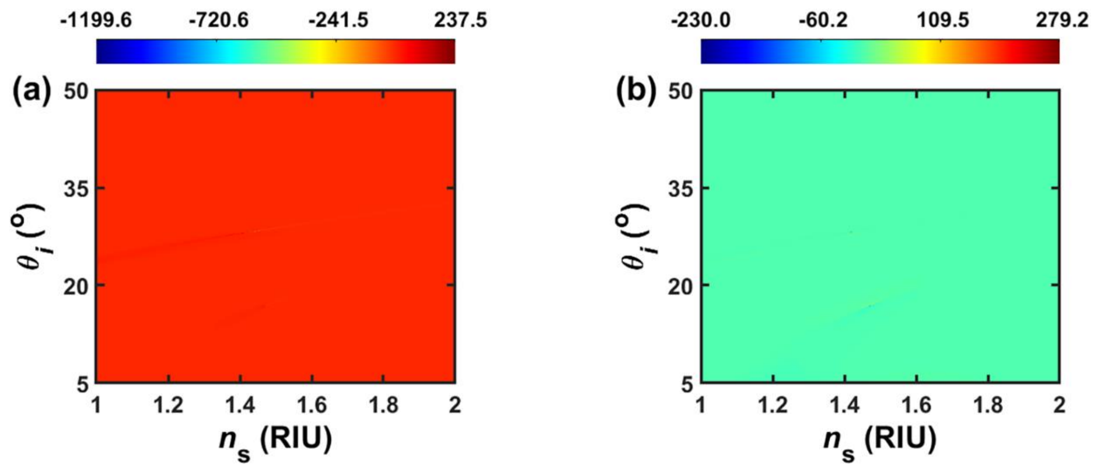

Fig. S4 Original color maps of Fig. 8(c) and (d). (a) In-plane and (b) transverse spin-dependent shifts versus the parameters of θ_i and n_s. The color bars are scaled in the unit of λ.

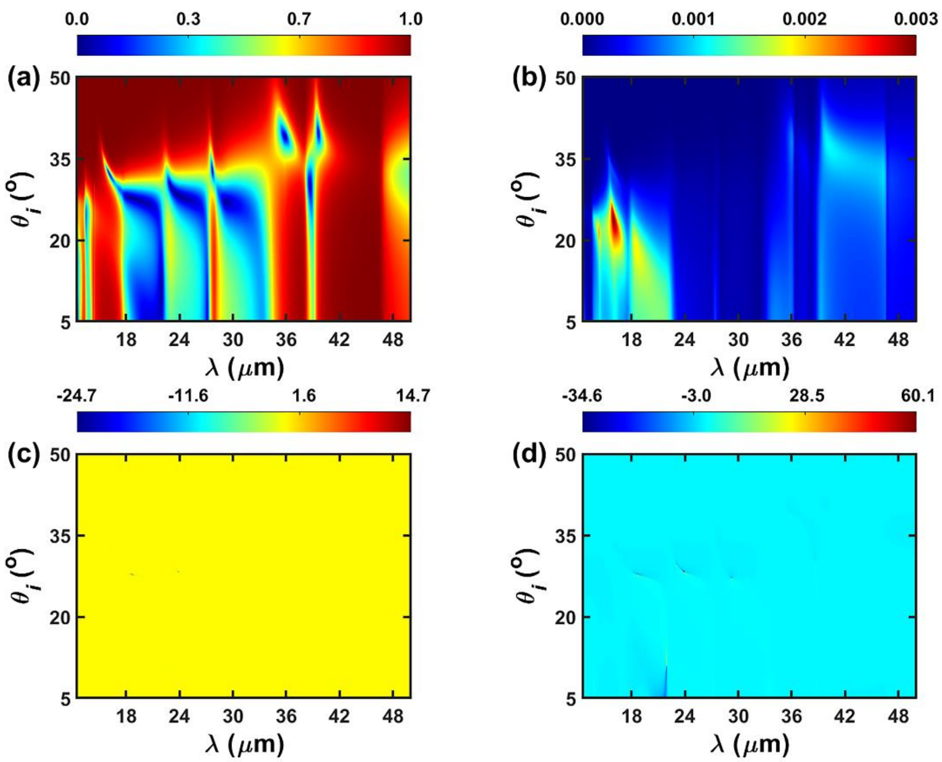

Fig. S5 Variations of the Fresnel reflection coefficients (a) $|r_{pp}|$and (b) $|r_{sp}|$ with respect to the incident angle θ_i and the wavelength λ of excitation light. (c) In-plane and (d) transverse spin-dependent shifts versus the parameters of θ_i and λ. The color bars in (a)(b) are unitless while they are scaled in the unit of λ in (c)(d). The off-diagonal permittivity element ε_{xy} of β-Ga_2O_3 is set to be zero, and all the other factors are the same with those of Figs. 3 and S1.

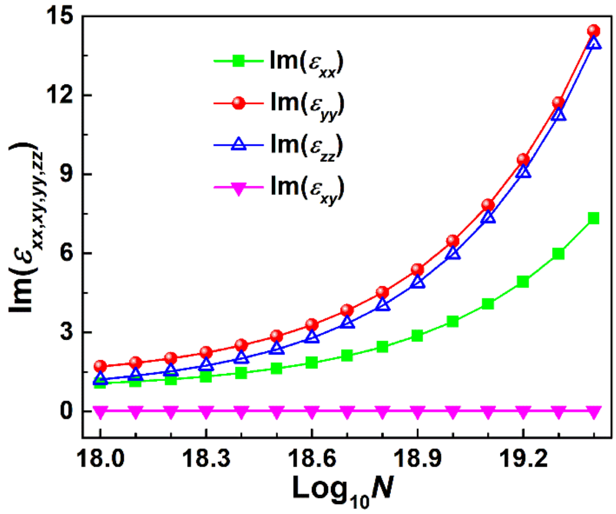

Fig. S6 Imaginary parts of permittivity elements ε_{xx}, ε_{yy}, ε_{zz} and ε_{xy} for the monoclinic β-Ga_2O_3 crystal at different doping concentrations N (in cm^{-3}). The wavelength is λ = 19.6 μm. The symbols are the practical data while solid lines are just drawn as a guide to the eye.

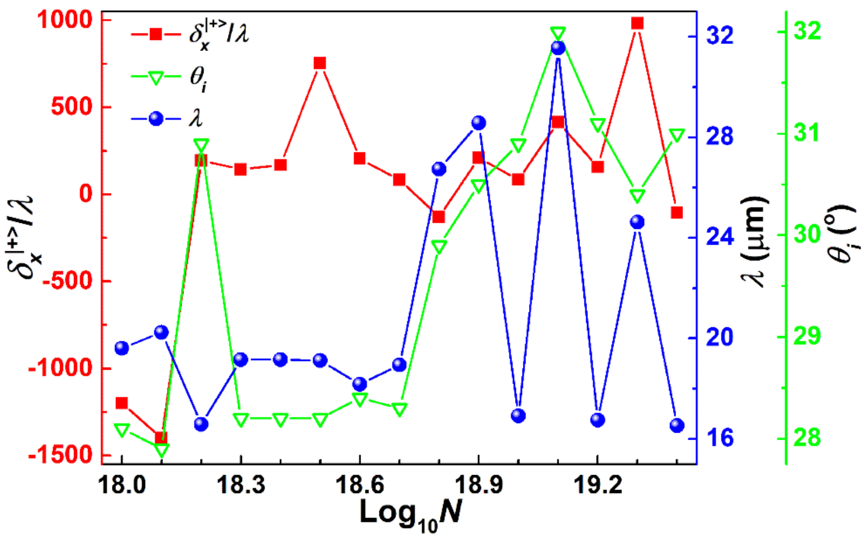

Fig. S7 The largest in-plane photonic spin Hall shifts and their corresponding θ_i and λ values for different $\log_{10}N$ values.

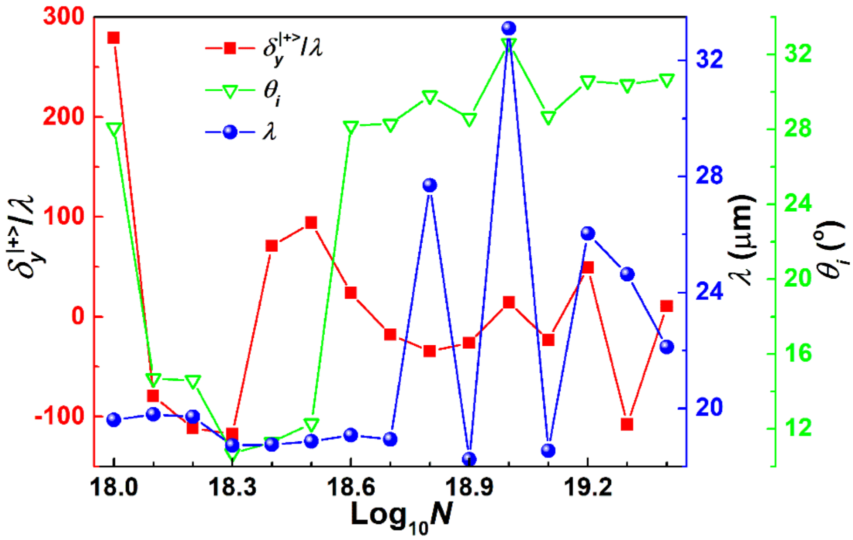

Fig. S8 The largest transverse photonic spin Hall shifts and their corresponding θ_i and λ values for different $\log_{10}N$ values.

Table S1 Real parts of permittivity tensor of β-Ga_2O_3 and the types of HShPs at different doping concentrations N in β-Ga_2O_3. The λ values correspond to the wavelengths at which in-plane photonic spin Hall shifts give their respective maximum displacements.

$Log_{10}N$	Frequency (cm^{-1})	λ (μm)	Re(ε_{xx})	Re(ε_{yy})	Re(ε_{zz})	Re(ε_{xy})	Types of HShPs
18.0	510	19.6	-4.5582	9.3249	-5.4666	-4.8064	Type II in-plane
18.1	494	20.2	-7.3034	7.0059	-8.9515	-5.123	Type II in-plane
18.2	603	16.6	-1.3175	-12.667	2.4216	3.5782	Type II out-of-plane
18.3	522	19.2	-4.2878	11.307	-4.0737	-4.9648	Type II in-plane
18.4	522	19.2	-4.8682	11.155	-4.2262	-4.9648	Type II in-plane
18.5	523	19.1	-5.4836	11.193	-4.2977	-4.9952	Type II in-plane
18.6	550	18.2	-3.2105	23.109	-1.9847	-7.7506	Type II in-plane
18.7	528	18.9	-6.954	11.928	-4.2746	-5.1954	Type II in-plane
18.8	374	26.7	-7.3795	0.47965	4.4136	8.2769	Type I in-plane
18.9	350	28.6	6.0318	9.6965	-1.2521	-8.5422	Type I out-of-plane
19.0	591	16.9	-9.8706	-22.336	-0.8027	5.5414	Elliptical
19.1	317	31.5	-28.758	-1.2121	-20.632	0.91674	Elliptical
19.2	597	16.8	-14.196	-19.613	-1.9577	4.3775	Elliptical
19.3	406	24.6	-16.114	0.99082	7.7346	9.3142	Type I in-plane
19.4	605	16.5	-21.075	-18.251	-3.8093	3.368	Elliptical

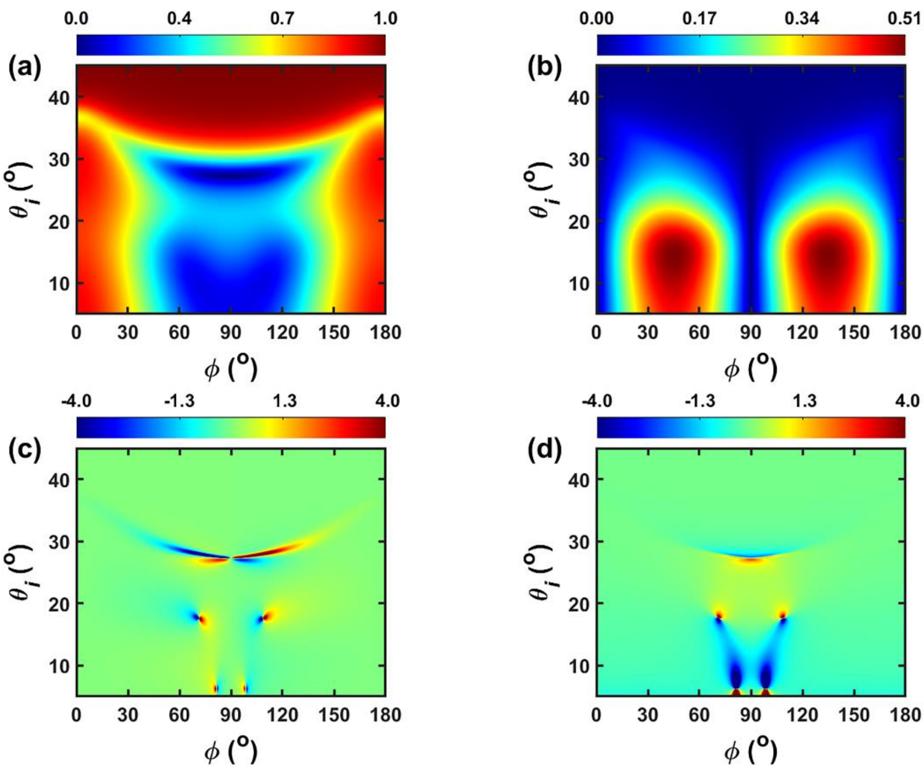

Fig. S9 Variations of the Fresnel reflection coefficients (a) $|r_{pp}|$and (b) $|r_{sp}|$ with respect to the incident angle θ_i and the azimuth angle ϕ. (c) In-plane and (d) transverse spin-dependent shifts versus the parameters of θ_i and ϕ. The color bars in (a)(b) are unitless while they are scaled in the unit of λ in (c)(d). The off-diagonal permittivity element ε_{xy} of β-Ga_2O_3 is set to be zero, and all the other factors are the same with those of Figs. 6 and S2.

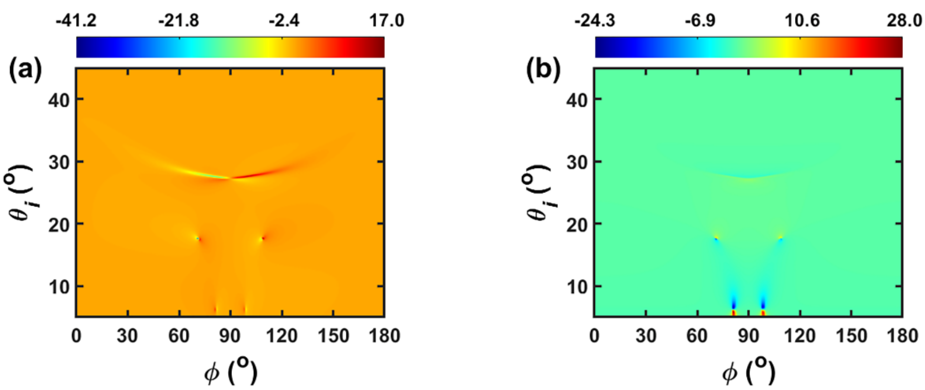

Fig. S10 Original color maps of Fig. S9(c) and (d). (a) In-plane and (b) transverse spin-dependent shifts versus the parameters of θ_i and ϕ at $\varepsilon_{xy} = 0.0$.